

## Effect of Stellar Scintillations on the Errors in Measuring the Ozone Content of the Atmosphere

A. V. Polyakov\*, Yu. M. Timofeev\*, A. S. Gurvich\*\*,  
V. V. Vorob'ev\*\*, V. Kan\*\*, and J.-H. Yee\*\*\*

\* *Research Institute of Physics, St. Petersburg State University,  
ul. Ul'yanovskaya 1, Petrodvorets, St. Petersburg, 198904 Russia*

\*\* *Oboukhov Institute of Atmospheric Physics, Russian Academy of Sciences, Pyzhevskii per. 3, Moscow, 109017 Russia*

\*\*\* *Johns Hopkins University, Applied Physics Laboratory, Johns Hopkins Rd. 11100, Laurel, Maryland, 20723-6099 USA*

Received February 24, 2000

**Abstract**—Methods and algorithms are developed for the numerical simulation of stellar scintillations in the atmosphere during satellite observations. Estimates of the accuracy of remote measurements of the ozone content in the atmosphere are obtained on the basis of the data on stellar radiation observed from space with allowance made for scintillations under different observation conditions. The dependence of the measurement accuracy on the spectral correlations of scintillations is studied. It is shown that a noticeable increase of errors in determining the ozone content is due to stellar scintillations and may reach, at least, a few percent. Such an increase is out of the limits of errors allowable nowadays in determining the gas content of the atmosphere. The methods of the numerical simulation of stellar scintillations and their consideration in determining the gas content from the results of satellite measurements of the atmospheric transparency require further development.

### INTRODUCTION

At present, the satellite systems of measuring of both the gas and aerosol contents of the atmosphere are the most important component of the global system of monitoring the atmospheric parameters [1–6]. Among numerous satellite methods, the method of determining the atmospheric transparency (hereinafter, the transparency method) on the basis of observations of the sun from space, which is based on the records of solar radiation absorption during sunsets and sunrises, holds a special place [5, 6]. The advantages of the method are its high potential accuracy, high vertical resolution, and relatively simple realization. However, the method's chief disadvantage is that the sun is used as a radiation source; hence, the number of measurement runs during 24 hours is small due to a limited orbital angular speed of a satellite. Thus, for example, the known SAGE-2, HALOE, and Ozone–Mir experiments allow one to take (over 24 hours) not more than 13–26 runs of measurements of the characteristics of the gas and aerosol state of the atmosphere at two slowly varying geographical latitudes [7–10]. Therefore, it takes a rather long time (about a month) to obtain the data of a global character with the aid of the measurements based on the observations of sunrises and sunsets.

The number of runs of measurements on the basis of the transparency method can be increased dramatically if stellar radiation is used. In this case, data can be obtained for different geographical regions from pole to pole at a high spatial resolution. In practice, the choice of a concrete set of the brightest stars restricts the num-

ber of measurement runs to a smaller number. For example, the authors of the experiment performed with the use of the UVISI instruments [11, 12] indicate 300 measurement runs during 24 hours, which is, nevertheless, an order of magnitude greater than the number of measurement runs taken during this period on the basis of the transparency method with the use of solar radiation. In the European GOMOS Project [13], which is to be realized in the near future, one can find even an estimate of 1600 measurement runs during 24 hours [14].

However, some additional problems arise in realizing the transparency method with the use of stellar radiation. First, it should be noted that small values of stellar radiation fluxes result in an increased importance of the fluctuations in the number of photons landing on the detector during the recordings or, in other words, in small values of the signal-to-noise ratio. Moreover, when observing stars through the atmosphere, one should take into account the effect of the real part of the air refractive index  $n$ . In the optical spectral region, the real part  $n - 1$  is proportional to the air density. Regular changes in  $n$  with height are responsible for a refraction decrease of the light flux from an observed star. Atmospheric turbulence results in refractive-index fluctuations and, as a consequence, in chaotic changes in the apparent stellar brightness. This latter phenomenon, which is usually called scintillation, plays the role of an additional multiplicative noise in measurements. Such noise may affect the accuracy in determining the characteristics of the gas content of the atmosphere.

While the photon statistics have been studied reasonably well, the effect of the multiplicative noise caused by stellar scintillations resulting from the atmospheric turbulence on the accuracy of atmospheric gas content measurements has been studied poorly. The theory describing turbulent scintillations has been developed in considerable detail and has passed evaluation tests in a number of measurements [15]. Space-based observations of stars through the earth's atmosphere were started by the Soviet cosmonauts [16]. The measurements described in [17, 18] have shown that, during observations from orbit at a height of 350 km, the frequency spectrum of stellar scintillations reaches a few kHz, and the modulation depth may exceed 100% when the minimum height of a sounding light ray is below 25–30 km. Averaging the data given in [18] over a time of 0.25–0.5 s, one can assure oneself that the residual turbulent fluctuations in light intensity may account for a few percent. This may result in a noticeable increase of errors in determining the atmospheric composition.

Therefore, it is evident that the effect of stellar scintillations must be taken into account in using stars as radiation sources in space-based measurements of the gas content of the atmosphere. In this paper, some estimates are given for the effect of stellar scintillations on the errors in retrieving the profiles of the ozone content. These estimates have been obtained on the basis of a numerical scintillation model developed by the authors. The properties of the model are based on the general theory of light propagation in the turbulent atmosphere, and the model's parameters have been chosen in accordance with the results of stellar scintillation observations from orbital stations.

#### REFRACTION IN A STAR EXPERIMENT— QUALITATIVE CONSIDERATION

This paper is apparently one of the first to be devoted to a quantitative analysis of the influence of refraction effects (regular and random) on the accuracy in determining the gas content of the atmosphere with the aid of the transparency method based on space observations of stars. Therefore, before the quantitative analysis, we shall give some qualitative considerations, which must clearly show the difference between the measurements based on the use of stars as radiation sources and the measurements based on the use of the sun or the moon as a radiation source.

The refractive index  $n - 1$  of the atmosphere decreases almost exponentially due to a decrease in air density [19]. During satellite observations at a height of a few hundreds or thousands of kilometers, one can model the refraction of light in the atmosphere by some negative cylindrical lens, neglecting the curvature of the planet's limb. The lower are the minimum ray heights, the greater is the divergence of light rays in free space behind the planet. Thus, refraction in the atmosphere results in a distortion of an observed image

of a star [20]. This refraction effect results simultaneously in an increase of the section of ray tubes and thus in a decrease of the radiation flux density; the longer is the distance from a ray's perigee, the less is the radiation flux density. However, the sun's image at the entrance slit of the spectrometer is locally decreased exactly as many times as the sections of ray tubes are changed ([21], the Helmholtz–Smith theorem). If the spectrometer's field of view is smaller than the image's size, the light flux falling on the detector will not change due to the presence of refraction in the atmosphere. A star's image is not resolved by the spectrometer's optical system during observations. As a result, the spectral radiation flux falling on the entrance objective lens of the spectrometer is a measured quantity.

Random inhomogeneities of the atmospheric refractive index can be viewed as a set of long-focus positive and negative lenses. At rather long distances, these lenses result in an increase or decrease of the radiation flux density. The results of stellar observations show that the flux density in local bursts due to random focusings may exceed its value for free space by several times [18]. This purely refraction effect is completely suppressed, if the spectrometer's entrance slit is smaller than the size of a source's image in it.

Inhomogeneities of the real part of the refractive index  $n$  are present in the atmosphere as well as the inhomogeneities of its imaginary part—the absorption coefficient. Moreover, both types of inhomogeneities may have a similar spatial structure. However, these two types of inhomogeneities show marked distinctions in the observed radiation. The observed effect of the inhomogeneities of the imaginary part is determined from the integral of the absorption coefficient along a ray. Therefore, the largest scale inhomogeneities exhibit the greatest effect, while small-scale inhomogeneities are not so important. This is, to a great extent, also true in respect to the attenuation due to (molecular and aerosol) scattering. The focusings and defocusings of radiation beyond the atmosphere due to the inhomogeneities of the refractive index are determined by two factors: the curvature of the phase front of the wave leaving the atmosphere and the distance between an observer and the atmosphere. One can roughly consider that the curvature of the phase front is proportional to the integral of the transverse (in respect to ray) Laplacian of the refractive index [22]. Therefore, scintillations are strongly dependent on small-scale inhomogeneities. A more strict consideration [15] shows that, for the Kolmogorov turbulence spectrum, for example, the low-frequency region of the scintillation spectrum is mainly determined by the smallest scale inhomogeneities of the refractive index.

Figure 1 shows the results of a qualitative consideration on the basis of the results of observations from the *Mir* orbital station. In the same figure, the results of measurements of the transmittances for the sun [9] and stars [18] are presented. Solar radiation was measured

by the Ozone–Mir instrument with an interval of 1 s; the measurement time was about 1 ms. The spectrometer’s optical system cut out a rectangle measuring  $1' \times 20'$  (the smaller size is for the vertical) on the sun’s image. Figure 1 gives the data for a wavelength of 459 nm and a spectral resolution of 0.5 nm. Star (the Canopus bright source) radiation was measured by an EFO-2 fast-response photometer with a sample frequency of 4096 Hz, at a wavelength of 480 nm with a band of 12 nm. To make comparing the data (obtained with such different space–time resolution) easier, the data obtained by the star photometer were averaged over time. The averaging interval was chosen so that, during the time of averaging, a stellar ray could change its height by the value corresponding to the height of the cutout made by the spectrometer aperture. As noted above, the measurements with the use of the sun as a radiation source are not subject to the refraction effects. Therefore, to compare the results of both the experiments, the results of measurements with the use of the sun were corrected through their multiplication by the refraction attenuation factor. This latter was calculated from the vertical distribution of air density on the basis of a standard model of the atmosphere. The mean variations of the transmittances are in good agreement with the data obtained from the observations of the two different sources, as could be expected. At the same time, the difference manifested by the presence of fluctuations on the curve plotted on the basis of star observations is pronounced. The time averaging suppresses very rapid scintillations with a modulation depth reaching 100%. However, the remaining low-frequency component (with a 5–10% amplitude) is a multiplicative noise in measuring the transmittances.

Note that, according to our estimates, the fluctuations in the figure cannot be explained by fluctuations in the radiation attenuation by the atmosphere, which is confirmed by a smooth curve obtained from the sun’s observations. The fluctuations remained after averaging are not caused by the shot noise, because this noise accounts for only 0.1–0.2% after the averaging.

#### REFRACTION IN THE STAR EXPERIMENT. STATEMENT OF THE PROBLEM AND NOTATION

During measurements of the atmospheric transparency on the basis of star observations, the atmosphere is scanned due to a satellite’s movement. We assume that the atmosphere does not change during the measurements. We also assume that the atmospheric refractive properties can be described by the refractive index  $N_\lambda = \text{Re}(n) - 1$ , which is proportional to the air density and is weakly dependent on the radiation wavelength  $\lambda$  [19]. The refractive index should be considered a random variable due to the presence of turbulence. We shall assume that its statistical mean  $\bar{N}_\lambda$  is the known function and is regularly dependent only on the height

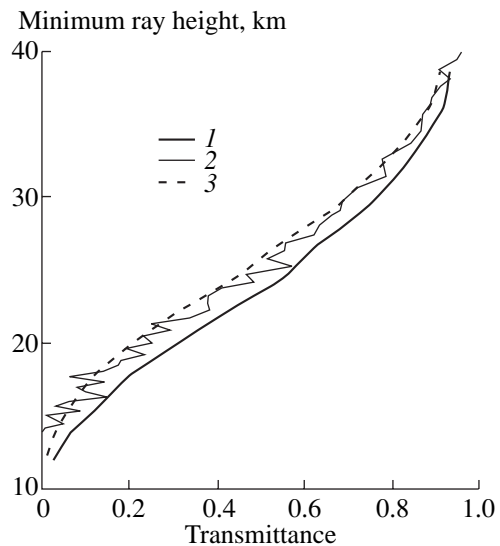


**Fig. 1.** Comparison between the results of measurements of the atmospheric transmittance with the use of the sun as a radiation source (1) with the Ozone–Mir instrument and with the use of the star as a radiation source (2) with the EFO-2 photometer from the *Mir* orbital station. Data (2) are obtained through averaging stellar scintillations over the time interval corresponding to one angular minute of the height averaging of the Ozone–Mir instrument. Curve (3) presents data (1) with a correction for a regular refraction decrease.

above the earth’s surface. Near the earth’s surface,  $\bar{N}_\lambda$  is about  $3 \times 10^{-4}$ . The turbulence-induced relative fluctuations  $(N_\lambda - \bar{N}_\lambda)/\bar{N}_\lambda$  in the atmosphere are weak and do not exceed a few percent, but the resultant fluctuations in stellar radiation (scintillation) can reach hundreds of percent during satellite observations. The spatial correlation functions of the refractive-index fluctuations or, which is the same, their spatial spectra will be assumed to be known.

The ray trajectory  $S(t, \lambda)$  corresponds to the time  $t$  and the wavelength  $\lambda$ . We shall assume that the trajectory is determined by a specified regular distribution of the air refractive index  $\bar{N}_\lambda$ . In the above assumption, the trajectory can be specified by the minimum ray height  $h(t)$  [22].

Regular variations in  $\bar{N}_\lambda$  with height result in the refractive attenuation of the radiation observed from a satellite. Let  $P_{\text{ref}}^F(h(t), \lambda)$  denote the regular refractive attenuation. The fluctuations in the refractive index result in random focusings and defocusings of observed stellar radiation. This effect (scintillation) will be characterized by the factor  $P_{\text{ref}}^{SC}(h, \lambda)$ . Its statistical mean is equal to unity. Let  $P_C(S(t, \lambda), \lambda)$  denote the radiation attenuation caused by the combined effects of molecular and aerosol scattering and gas absorption along the ray. Then, the intensity  $I(t, \lambda)$  of stellar radiation pass-

ing through the atmosphere and reaching the instrument's entrance aperture is described by the following equation:

$$I(t, \lambda) = I_{\text{star}}(\lambda) P_{\text{ref}}(t, \lambda) P_C(S(t, \lambda), \lambda). \quad (1)$$

Here,  $I_{\text{star}}(\lambda)$  is the intensity of stellar radiation incident on the atmosphere,

$$P_{\text{ref}}(t, \lambda) = P_{\text{ref}}^{SC}(t, \lambda) P_{\text{ref}}^F(t, \lambda). \quad (2)$$

The instrument performs the measurement of the energy of radiation passing through its entrance aperture in a finite time interval  $\Delta t$ . The typical values for the time taken to integrate signals are between 0.25 and 0.5 s, which correspond to sensor Nyquist frequencies of a few Hz. In the approximation under consideration, there is a one-to-one correspondence between the time and the minimum ray height, which allows us to replace the time dependence by the height dependence. For the integration time indicated above, the height is decreased by about 1 km.

With that notation made, the value of  $I(\Delta t, \lambda)$  measured over the signal integration period  $\Delta t$  is described by the equation:

$$\begin{aligned} & I(\Delta t, \lambda) \\ &= I_{\text{star}}(\lambda) \frac{1}{\Delta t} \int_{\Delta t} P_{\text{ref}}^{SC}(t, \lambda) P_{\text{ref}}^F(t, \lambda) P_C(S(t, \lambda), \lambda) dt. \end{aligned} \quad (3)$$

Instead of the absolute signal value  $I(\Delta t, \lambda)$ , it is convenient to consider the atmospheric transmittance  $P(\Delta t, \lambda)$ :

$$P(\Delta t, \lambda) = \frac{I(\Delta t, \lambda)}{I_{\text{star}}(\lambda)}. \quad (4)$$

Then, from expressions (3.3) and (3.4), one can obtain:

$$\begin{aligned} & P(\Delta t, \lambda) \\ &= \frac{1}{\Delta t} \int_{\Delta t} P_{\text{ref}}^{SC}(t, \lambda) P_{\text{ref}}^F(t, \lambda) P_C(S(t, \lambda), \lambda) dt. \end{aligned} \quad (5)$$

Let  $P_{\text{atm}}(S(t, \lambda), \lambda)$  denote the product of the slowly varying integrand functions  $P_{\text{atm}}(S(r, \lambda), \lambda) = P_{\text{ref}}^F(t, \lambda) P_C(S(t, \lambda), \lambda)$ , and expression (5) will be represented in the following form:

$$P(\Delta t, \lambda) = \frac{1}{\Delta t} \int_{\Delta t} P_{\text{ref}}^{SC}(t, \lambda) P_{\text{atm}}(S(t, \lambda), \lambda) dt. \quad (6)$$

In expression (6), the rapidly varying function  $P_{\text{ref}}^{SC}(h, \lambda)$  and the slowly varying (in the integration interval)

function  $P_{\text{atm}}(S(t, \lambda), \lambda)$  are under the integral. Hence, the following approximate equation is valid:

$$\begin{aligned} P(\Delta t, \lambda) &\approx \frac{P_{\text{atm}}(S(t_0, \lambda), \lambda)}{\Delta t} \int_{\Delta t} P_{\text{ref}}^{SC}(t, \lambda) dt \\ &t_0 \in [t, t + \Delta t]. \end{aligned} \quad (7)$$

The wavelength dependence of the refractive index is rather weak. However, this dependence results in different minimum ray heights corresponding to different wavelengths. The difference in the minimum ray heights is small. For example, for the wavelengths of 600 and 900 nm, this difference may account for about 100 m at a height of 10 km and decreases exponentially with height. However, the chromatic effects influence the scintillation correlation in the different regions of the observed radiation spectrum [23, 24].

## METHODS OF STELLAR SCINTILLATION SIMULATION

For the analysis of the refraction effects causing observed stellar scintillations in the occultation experiments, the method of an equivalent phase screen [22], which replaces the effect of the field of the real part of the atmospheric refraction index on propagating radiation, is an appropriate approximation. The phase disturbances in the screen include a regular part resulting from the regular changes in the refractive index with height with a characteristic scale of the order of the homogeneous atmosphere height and also a random part resulting from the turbulent fluctuations in the refractive index.

The turbulence properties have been much studied only for the atmospheric boundary layer, where, according to the results of many measurements, the Kolmogorov isotropic turbulence is dominating. In the stratosphere, a strongly stable thermal stratification is favorable for forming strongly anisotropic stratified inhomogeneities. An analysis of the measurements [17, 25] showed that the observed stellar scintillations are mainly due to the inhomogeneities whose characteristic horizontal dimensions are tens of times greater than their vertical dimensions. According to the estimates given in [17, 25] and the data obtained from the aerostat sounding [26, 27], the vertical spectrum of the refractive index inhomogeneities can be approximated by the power-law dependence with the exponent  $-3$ . According to the results of many observations [15], the probability distribution of the relative intensity fluctuations is well described by a log-normal law. For such strongly anisotropic inhomogeneities, the model of a one-dimensional screen, in which both variations (regular and random) occur only vertically, can be used as an equivalent phase screen.

In this work, the numerical simulation of stellar scintillations is based on the assumption that the turbulent fluctuations of an observed light flux follow the

log-normal distribution. In addition to the distribution law, the following characteristics were assumed to be known:

(1) The dependence of the variance of relative fluctuations in the light intensity at the minimum ray height  $h$ :

$$\beta^2(h) = \frac{\overline{I^2(h)}}{\overline{I(h)}^2} - 1, \text{ where } \overline{I(h)} = I_{\text{star}}q(h) \text{ are the varia-}$$

tions in intensity with height, resulting from regular refraction, and  $q(h)$  is the regular refraction attenuation calculated on the basis of the standard atmosphere model. The overlined bar denotes the mean value.

(2) The one-dimensional spectrum of the relative fluctuations in the logarithm of the light wave intensity  $\chi(h) = (1/2)\ln(I(h)/\overline{I(h)})$ . As a function of the vertical wave number  $p$ , this spectrum is given in the form

$$V_\chi(h, p) = \frac{1}{2}\sigma_\chi^2(h)[V_0(r_1(h), p) + V_0(r_2(h), p)], \quad (8)$$

$$V_0(r, p) = \frac{3}{2\sqrt{\pi}} \frac{r}{(rp)^4} \sin^4[(rp)^2],$$

$$\sigma_\chi^2(h) = \frac{1}{4} \ln[1 + \beta^2(\beta_0(h))], \quad (9)$$

$$\beta^2(\beta_0) = [1 - \exp(-\beta_0^2) + C0\beta_0^4 \exp(-(\beta_0 - 1)^2)],$$

where

$$\beta_0^2(h) = 4C_i^2 \overline{N(h)}^2 k^2 r_F^3(h), \quad r_F(h) = \sqrt{\frac{L}{2k}} q(h) \quad (10)$$

is the Fresnel size;

$$r_1(h) = \frac{r_F}{1 + C1\beta_0(h)} \quad \text{and} \quad (11)$$

$$r_2(h) = r_F(h)(1 + C2\beta_0(h))$$

are two scales of the spectrum of fluctuations in the amplitude logarithm;  $\overline{N(h)}$  is the height profile of the refractive index according to the standard atmosphere model; and  $C_t$ ,  $C_0$ ,  $C_1$ , and  $C_2$  are the fitting coefficients. The spectrum form chosen by us agrees with the measurement data given in [18] and the theoretical conceptions presented in [28].

For spectrum (8), the relationships  $\int_{-\infty}^{\infty} V_0(r, p) dp = 1$  and  $\int_{-\infty}^{\infty} V_\chi(h, p) dp = \sigma_\chi^2(h)$  are fulfilled. The form of this spectrum is chosen on the basis of the following requirements. Under weak fluctuations, when  $\beta_0(h) \ll 1$  and  $r_1(h) = r_2(h) = r_F(h)$ , the spectrum  $V_\chi(h, p)$  corresponds to the spectrum of fluctuations behind the phase screen with the power-law phase-fluctuation spectrum  $V_\varphi(h, p) \sim \overline{N(h)}^2 p^{-4}$  or to anisotropic inhomogeneities of the refractive index with the vertical spectrum with the exponent  $-3$ . In this case, the spectrum  $V_\chi(h, p)$  is

determined by one spatial scale  $r_F$ . In the region of strong fluctuations, with an increase of the parameter  $\beta_0(h)$ , the spectrum  $V_\chi(h, p)$  becomes two-dimensional [28]; in this case, if  $\beta_0(h) \gg 1$ , the smaller spatial scale  $r_1$  must be of the order of the coherence radius  $r_c(h)$ , and the larger scale  $r_2$  must be of the order of the ratio  $r_F^2/r_1$ . Since, in the region of strong fluctuations, the coherence radius is smaller than or of the order of the Fresnel size, which is about 1 m for the optical spectral region, i.e., smaller than the inner scale of strongly anisotropic turbulence, the scale  $r_c(h)$  must be inversely proportional to the value of  $\beta_0(h)$  in accordance with the first formula in (11). The fitting coefficients were chosen so that an agreement could be achieved between the simulated and actual scintillations.

The algorithm of scintillation simulation involves following three procedures. In the first one, with the aid of the method of spectral filtering [29], the portions of the one-dimensional refractive-transmittance realizations observed at the distance  $L$  from the phase screen are generated as functions of the minimum ray height  $h$  with a step of 7 cm. Within each of the portions (2 km in length), the intensity fluctuations are assumed to be homogeneous and log-normal and to have the spectrum determined from Eqs. (8)–(10). Then, the realizations are corrected with the aid of splines within these portions, and a general realization with a smooth dependence of the mean parameters is obtained.

The second procedure involves the recalculation of the height refractive-transmittance profiles into the time dependences for the given wavelength  $\lambda$  and the given observation time  $t$  with allowance for a concrete measurement geometry characterized by the angle  $\alpha$  between the satellite's orbit axis and the direction to the star. In this case, the dispersion of the refractive index was taken into account through the dependences of the refraction angles on the wavelength  $\lambda$ . The chromatic dispersion results in a regular time (or height) shift among the realizations at different wavelengths, which increases with an increase of the difference in wavelengths and with a decrease of the height  $h$ . This dispersion shift is the main reason for the chromatic decorrelation of the realizations simulated at different radiation wavelengths.

The third procedure imitates the process of averaging the realizations of the refractive transmittance under real measurements with a finite time of signal integration.

The comparison between the model scintillation realization and the measured one given in [18] shows their qualitative agreement. However, there are some differences caused by the limitations of the numerical model. First, these limitations are due to the neglect of the Kolmogorov isotropic turbulence contribution to simulated scintillations. In particular, this results in an increased correlation of the simulated realizations at different wavelengths [24]. Moreover, an analysis of

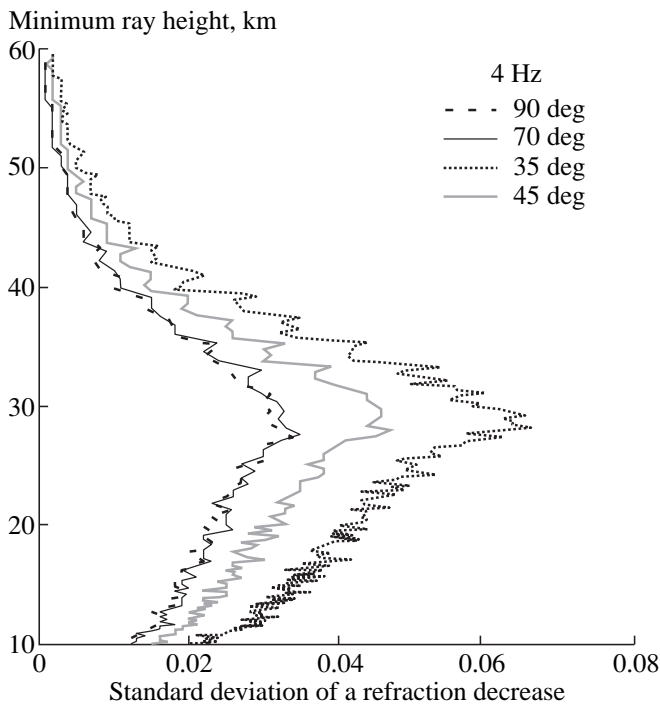


**Fig. 2.** Results of numerical simulation of random scintillation realizations—the rms variability of the refractive transmittance at an sampling frequency of 4 Hz (the curves are marked by the value of the angle  $\alpha$ ).

scintillations averaged over the time 0.25–0.5 s shows that the model scintillations in the region of strong fluctuations (at heights below 25–30 km) are smaller in value than the appropriately averaged experimental scintillations. This is apparently due to an incomplete adequacy of the spectrum (8) in the region of strong scintillations.

The indicated limitations of the model can lead to an underestimation (more significant at heights below 30 km) of the errors in reconstructing the ozone content. Nevertheless, the methods developed and the scintillation realizations modeled indicate that an allowance for the effect of stellar scintillations on the accuracy of retrieving the ozone content is of fundamental importance and can be used for preliminary estimates of the retrieval errors due to stellar scintillations.

#### STATISTICAL SIMULATION OF SCINTILLATIONS

To obtain the statistical characteristics of scintillations with the use of the methods described above, 300 random realizations of the profile of the average refractive transmittance  $\tilde{P}_{\text{ref}}(h, \lambda)$  were calculated. The calculations were performed for a few values of the angle  $\alpha$  between the orbit axis and the direction to the star for the measurements with a frequency of 2 and 4 Hz (we neglect the time taken to inquire the receiver, therefore, for example, the time of signal integration

500 ms corresponds to a frequency of 2 Hz) in the spectral range between 580 and 900 nm with a width of 10 nm.<sup>†</sup> On the basis of the data obtained, the mean  $\bar{P}_{\text{ref}}(h, \lambda_i)$  and the spectral covariance scintillation matrices  $\Sigma_{\text{sc}}(h) = \{\sigma_{i,j}\}_{i,j=1,m}$  for different minimum ray heights were calculated:

$$\bar{P}_{\text{ref}}(h, \lambda_i) = E\tilde{P}_{\text{ref}}(h, \lambda_i);$$

$$\sigma_{i,j} = E(\tilde{P}_{\text{ref}}(h, \lambda_i) - \bar{P}_{\text{ref}}(h, \lambda_i))(\tilde{P}_{\text{ref}}(h, \lambda_j) - \bar{P}_{\text{ref}}(h, \lambda_j));$$

here,  $E$  is the symbol of mathematical expectation, which is taken according to the modeled random realizations of  $\tilde{P}_{\text{ref}}(h, \lambda_i)$ .

Figure 2 shows some examples of the calculated height dependences of the rms deviations  $s_1(h) = \sqrt{\sigma_{1,1}}$  characterizing the variability of the coefficients of refractive transmittance for an sampling frequency of 4 Hz for different observation geometries. The value of  $s_i(h)$  changes slightly with the wavelength. The oscillations of the curves in Fig. 2 are due to the model's properties. The fact that the oscillation values are noticeably smaller than the values of the rms deviations allows us, at a first approximation, to consider this model appropriate for a statistical analysis of scintillations. In Fig. 2, one can see an expected dependence of the refractive transmittance variability, which increases with an increase of  $\alpha$ , because the thickness of averaging layers decreases. Height variations in refractive transmittance have a maximum of about 30 km, which is explained by the combination of an increase of the scintillation amplitude due to an increased refractive index and a decrease of the regular refractive transmittance due to a decreased height.

As for the problem of retrieving the profiles of gas content of the atmosphere, signal variability due to scintillations makes up an additional multiplicative noise; height variations in the value of this noise are shown in Fig. 2. With allowance made for the errors in measurements taken by modern instruments (purely instrumental noise component is 0.1–1% of absolute transmittance; the quantum noise, which is significantly different for stars of different stellar magnitudes, is not considered here), it is seen that the noise contributed by scintillations may noticeably exceed the instrumental errors, which confirms the importance of a correct allowance for scintillations in interpreting the results of measurements of the atmospheric transparency.

The height variations in the coefficient of correlation between the results of measurements taken at wavelengths of 580 and 900 nm for different observation geometries are shown in Fig. 3. It is seen that, for the model of scintillations that was used, the correlation

<sup>†</sup> This spectral range is used in the SPIM-5 spectrometer operating now as a part of the UVISI instrumentation on board the MSX satellite [12].



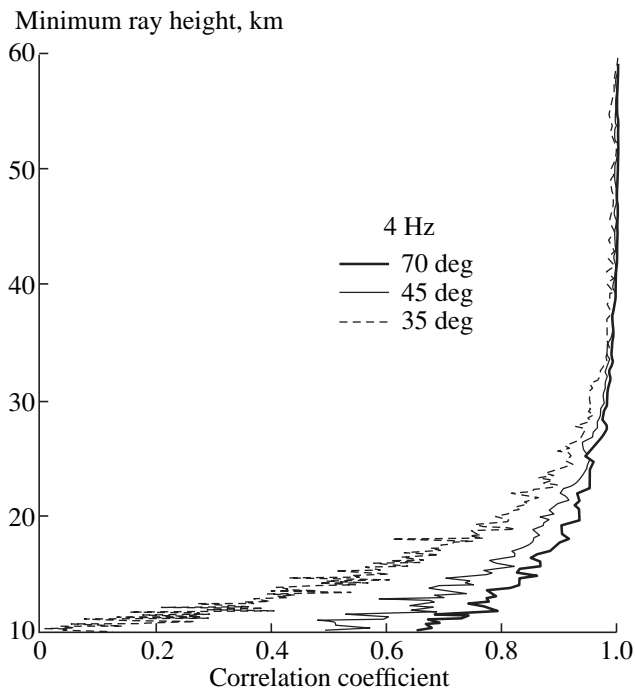


**Fig. 3.** Height variations in the coefficient of correlation of scintillations at wavelengths of 900 and 580 nm, an sampling frequency of 4 Hz, and  $\alpha = 70^\circ, 45^\circ,$  and  $35^\circ$ . The curve for  $\alpha = 90^\circ$  is not shown, because it is overlapped by the curve for  $\alpha = 70^\circ$ .

coefficients are close to unity up to the heights of the order of 20 km, and then they decrease sharply. This decrease is especially sharp at small angles  $\alpha$ . At a height of 10 km and at  $\alpha = 35^\circ$ , correlation is almost lacking.

Figure 4 (solid lines) gives the spectral dependence of the correlation coefficient for different wavelengths at  $\alpha = 35^\circ$ , an sampling frequency of 4 Hz, and a minimum ray height of 10 km. This combination of the parameters results in the value 0.15 for the correlation coefficient for the boundaries of the interval under consideration. For all other alternative calculations, the correlation coefficient value is larger. Figure 4 shows that the spectral dependence of the correlation coefficients is close to the linear one. In fact, in analyzing the mechanism of occurrence of correlations in the model considered for scintillations, one can easily understand that the correlation coefficient depends linearly on the dispersion shift in the minimum ray height for different wavelengths, which is confirmed by the behavior of the curves in Fig. 4.

With the aid of the method of statistical simulation, the covariance matrices can be obtained only for a specific set of wavelengths. To generalize the calculation results to arbitrary wavelengths, we can use a simple linear (in the refractive index) approximation:

$$\Sigma_{sc} = \{\sigma_{i,i}\}_{i,j=1,m} \sigma_{i,j} = s_i s_j (k_{1,m} \text{abs}(n_i - n_j) + 1 (\text{abs}(n_1 - n_m) - \text{abs}(n_i - n_j)) / \text{abs}(n_1 - n_m)); \quad (12)$$

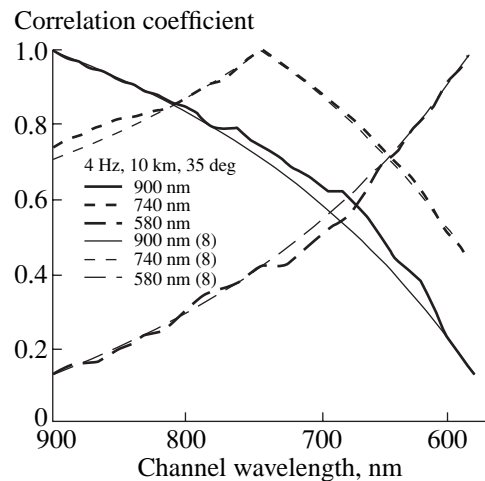


**Fig. 4.** Spectral variations in the correlation coefficient at  $\alpha = 35^\circ$  for three wavelengths, an sampling frequency of 4 Hz, and a minimum ray height of 10 km. Solid lines denote the results of the statistical numerical simulation, and thin lines denote the results of calculations on the basis of (12).

here,  $m$  is the number of a spectral channel;  $n_i, n_j, n_1,$  and  $n_m$  are the air refraction indices for the channels with the corresponding numbers;  $k_{1,m}$  is the correlation coefficient for the most distant (in spectrum) pair of channels (the channels' wavelengths are assumed to be ordered); and  $s_i = s(\lambda_i)$  is the rms variation of the refractive transmittance. The values of  $s$  and  $k_{1,m}$  were calculated earlier for different heights.

Figure 4 (thin lines) shows the correlation coefficient calculated on the basis of (12). It is seen that the results of the numerical statistical simulation and the results of calculations on the basis of (12) are in good agreement, which allows us to use this approximation below.

As noted above (see the description of the scintillation model), the model used for scintillations overestimates the correlations between signal scintillations at different wavelengths. To demonstrate the need for a more detailed study of the behavior of the spectral correlations of scintillations, in parallel with the correlation matrices given above, we shall consider an exponential model of the covariance matrix:

$$\Sigma_{sc} = \{\sigma_{i,j}\}; \quad \sigma_{i,j} = s_i s_j \exp\left(-\frac{|\lambda_i - \lambda_j|}{r}\right), \quad (13)$$

where  $r$  is the spectral correlation radius.<sup>2</sup>

<sup>2</sup> We do not assume that the real scintillations have spectral correlations like those in (13), and consider this case only to illustrate that the character of spectral correlations significantly affects the errors in determining gas-content profiles.

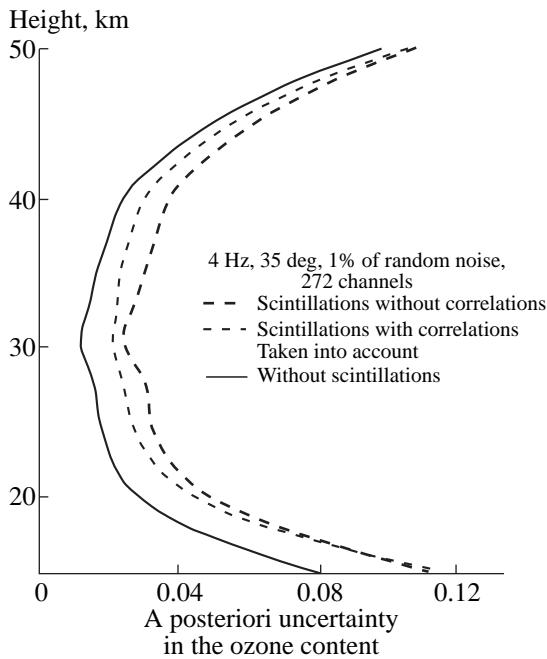


**Fig. 5.** Estimates of errors in retrieving the ozone profile with allowance for scintillation “noise.”

#### ESTIMATIONS OF ERRORS IN RETRIEVING OZONE CONTENT PROFILES

In the foregoing, we have considered the noise caused by the variations in refractive transmittance in multiplicative form. For further analysis, it is convenient to switch to the additive form of its presentation. Let us introduce the following notation:

$\tilde{P}_{\text{ref}}^{SC}(\Delta t, \lambda) = \frac{1}{\Delta t} \int_{\Delta t} P_{\text{ref}}^{SC}(t, \lambda) dt$  are the scintillations averaged over the time  $\Delta t$ ;

$\tilde{P}_{\text{ref}}(\Delta t, \lambda) = \frac{1}{\Delta t} \int_{\Delta t} P_{\text{atm}}(S(t, \lambda), \lambda) dt$  is the average atmospheric transmittance.

Both experiments and our above estimates show that  $\hat{P}_{\text{ref}}^{SC}(h, \lambda)$  differs slightly (only a few percent) from unity for a typical value of the averaging time. Let us rewrite (7) in a somewhat different form:

$$P(h, \lambda) \approx \tilde{P}_{\text{ref}}^{SC}(h, \lambda) \tilde{P}_{\text{atm}}(h, \lambda) \quad (14)$$

or

$$P(h, \lambda) \approx \tilde{P}_{\text{atm}}(h, \lambda) + (\tilde{P}_{\text{ref}}^{SC}(h, \lambda) - 1) \tilde{P}_{\text{atm}}(h, \lambda). \quad (15)$$

We shall consider the addend in (15) as the additive noise  $\varepsilon_{\text{ref}}(\lambda_i)$  whose characteristics can be determined

from a numerical statistical simulation of scintillations:

$$E\varepsilon_{\text{ref}}(\lambda_i) = 0, \quad \Sigma_{SC}^A = \{\sigma_{i,j}^A\}, \quad (16)$$

$$\begin{aligned} \sigma_{i,j}^A &= E\varepsilon_{\text{ref}}(h, \lambda_i)\varepsilon_{\text{ref}}(h, \lambda_j) \\ &= \sigma_{i,j} \frac{\tilde{P}_{\text{atm}}(h, \lambda_i)\tilde{P}_{\text{atm}}(h, \lambda_j)}{\tilde{P}_{\text{ref}}^F(h, \lambda_i)\tilde{P}_{\text{ref}}^F(h, \lambda_j)}. \end{aligned}$$

The following estimates of errors in retrieving the ozone content are based on a well-known relationship for the residual covariance matrix of the uncertainty of a reconstructed profile of atmospheric parameters [30]:

$$\hat{D} = (A'\Sigma^{-1}A + D^{-1})^{-1}. \quad (17)$$

Here,  $D$  is the a priori covariance matrix of the vector of atmospheric parameters;  $\hat{D}$  is the a posteriori covariance matrix, i.e., the matrix of the residual uncertainty of this vector;  $A$  is the kernel of the direct-problem operator; and  $\Sigma$  is the covariance matrix of the total noise of measurements

$$\Sigma = \Sigma_{SC}^A + \Sigma_{\varepsilon}, \quad (18)$$

where  $\Sigma_{\varepsilon}$  is the covariance matrix of the measurement noise. The errors in retrieving the ozone profile were calculated for the linear (12) and exponential (13) covariance matrices  $\Sigma_{SC}$ . It was assumed in the calculations that 272 channels in the spectral range between 580 and 900 nm were used to determine the ozone profile (the SPIM-5 spectrometer in the experiment [11, 12]). Radiation absorption by ozone,  $\text{NO}_2$ , and  $\text{NO}_3$ ; attenuation due to molecular and aerosol scattering; and variabilities of all these components were taken into account. Generally, it is difficult to estimate the random noise  $\Sigma_{\varepsilon}$  produced by other factors, because this noise is determined by many factors—the characteristics of the stars, instruments, and the methods used to obtain the transmittance (in particular, correction of night airglow). Therefore, for our estimates, we used the value of the rms deviation of noise equal to 1% of absolute transmittance and assumed that its spectral and height correlations are lacking. Errors were considered in retrieving the ozone profile with a vertical averaging of 1 km. A relative a priori variability of the ozone profile for all the heights and that of other atmospheric parameters were assumed equal to 60 and 100%, respectively.

The estimates of errors in reconstructing the ozone profile are given in Fig. 5 for the cases without scintillations, with linear correlations in spectrum, and with scintillations noncorrelated in spectrum. It is seen that an additional “noise” of scintillations increases the error in determining the profile of ozone content by 1.5–2 times or by 1–3% of a relative error in the height range between 10 and 40 km. Since, at present, high requirements are imposed upon the accuracy in determining the ozone content [3, 5, 7], this increase should be considered significant. Moreover, the effect of scin-



tillations is especially significant for the model that does not take into account the presence of spectral correlations.

The calculations of errors for the exponential covariance matrix at different values of the spectral correlation length are given in Fig. 6. We have presented the results for heights below 30 km, because, at higher altitudes, the above model describes the spectral scintillation correlations reasonably well. (In Fig. 5, the curve “without correlations” corresponds to the case  $r = 0$ .) As seen from Fig. 6, errors in retrieving the ozone profiles increase as the spectral correlation length  $r$  decreases. It should be noted that, in our calculations, the correlation length does not depend on height, which is a rough approximation.

Figure 6 shows that, under the assumption that the matrix of spectral correlations has an exponential form, the errors in retrieving the ozone profile may increase by more than two times due to the scintillation “noise,” i.e., by 10% of a relative error for heights of 10–15 km. This points to the fact that it is necessary to develop the methods taking into account the effect of stellar scintillations, the models of scintillations, and the studies of (first of all) the spectral correlation structure of stellar scintillations.

The above estimates are obtained under the assumption that the statistical scintillation characteristics used in radiation measurements correspond to the real ones occurring in the atmosphere in the course of the measurements. An improvement of the model of scintillations will result in changes of estimated errors. Moreover, in this work, we have not considered the effect of such an important factor as a shot (quantum) measurement noise caused by a the low intensity of star radiation. Taking into account this effect, one should note that the brighter a star is, the more important the role of multiplicative turbulent noise is (in respect to other measurement noises).

## CONCLUSIONS

The problem of space occultation experiments on the study of the gas content of the atmosphere with allowance for stellar scintillations is formulated. A model is proposed to imitate stellar observations from space through the atmosphere. Stellar scintillations are statistically simulated with the aid of the model proposed.

It is shown that the effect of stellar scintillations may result in a noticeable decrease (at least, by a few percent) of the accuracy in determining the ozone content on the basis of the method of measuring the atmospheric transparency through stellar scintillations. Since, at present, high requirements are imposed upon the accuracy in monitoring the ozone content of the atmosphere, this decrease is significant.

On the basis of an exponential spectral covariance matrix, it is shown that the form of spectral variations

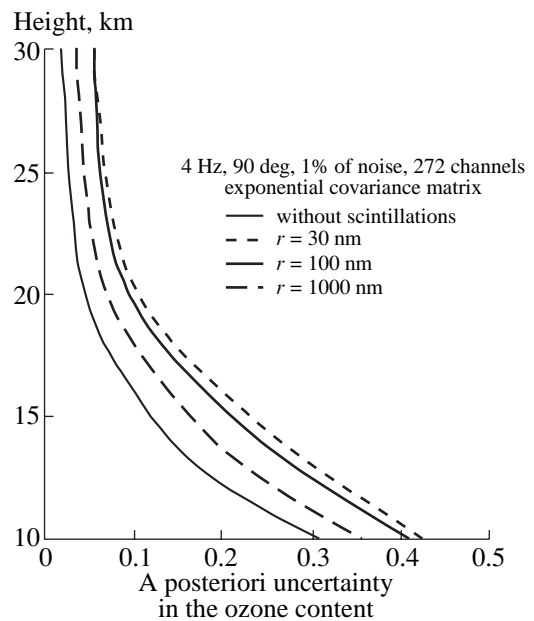


**Fig. 6.** Estimates of errors in retrieving the ozone profile with allowance for the “noise” of stellar scintillations with an exponential covariance matrix.

in scintillation correlations significantly affects the errors of remote sounding. From this follows the conclusion that it is necessary to develop the studies of the effect of stellar scintillations on the errors in measuring the atmospheric transparency through stars and especially to study the spectral behavior of stellar correlations.

A specific spectrum-correlated character of noise contributed by stellar scintillations to the results of measurements requires the development of special approaches to take into correct account and to parametrize this noise in the inversion of transparency measurements.

## ACKNOWLEDGMENTS

The work was supported by the Russian Foundation for Basic Research, project nos. 98-05-64717, 97-05-65492, and 97-02-16894.

## REFERENCES

1. Dozier, J., Planned EOS Observation of the Land, Ocean and Atmosphere, *Atmos. Res.*, 1994, vol. 31, pp. 329–357.
2. *Global Climate Observing System. GCOS/GTOS Plan for Terrestrial Climate-Related Observation. Version 1.0 (1995): GCOS-21. WMO/TD*, Geneva: WMO, 1995, no. 721.
3. *WMO, Plan for Space-Based Observation. Global Climate Observing System, GCOS-15. WMO/TD*, Geneva: WMO, 1995, no. 684.

4. *CEOS Yearbook, 1997. Committee on Earth Observation Satellites: Towards an Integrated Global Observing Strategy*, European Space Agency, 1997.
5. Karol', I.L., Rozanov, V.V., and Timofeev, Yu.M., *Gazovye primesi v atmosfere* (Gas Admixture in the Atmosphere), Leningrad: Gidrometeoizdat, 1983.
6. Timofeev, Yu.M., *Satellite Methods of Gas Composition Studies in the Atmosphere*, *Izv. Akad. Nauk SSSR, Fiz. Atmos. Okeana*, 1989, vol. 25, no. 5, pp. 451–472.
7. McCormick, M.P., *SAGE 2: An Overview*, *Adv. Space Res.*, 1987, vol. 7, no. 2, pp. 73–86.
8. Russel, J.M.III., Gordley, L.L., Park, J.H., Drayson, S.R., Hesketh, W.D., Cicerone, R.J., Tuck, A.F., Frederick, J.E., Harrieres, J.E., and Crutzen, P.J., *The Halogen Occultation Experiment*, *J. Geophys. Res. D*, 1993, vol. 98, no. 6, pp. 10 777–10 797.
9. Poberovskii, A.V., Polyakov, A.V., Timofeev, Yu.M., Kovalev, A.E., Prokhorov, V.M., Khrustalev, A.Z., Panchenko, V.A., Mansurov, I.I., and Volkov, O.N., *Ozone Profile Determination by Occultation Sounding from the Mir Space Station: 1. Instrumentation and Data Processing Method*, *Izv. Ross. Akad. Nauk, Fiz. Atmos. Okeana*, 1999, vol. 35, no. 3, pp. 312–321 [*Izv., Atmos. Ocean. Phys.* (Engl. Transl.), 1999, vol. 35, no. 3, pp. 282–290].
10. Polyakov, A.V., Poberovskii, A.V., and Timofeev, Yu.M., *Ozone Profile Determination by Occultation Sounding from the Mir Space Station: 2. Comparison of the Observational Results with Independent Data*, *Izv. Ross. Akad. Nauk, Fiz. Atmos. Okeana*, 1999, vol. 35, no. 3, pp. 322–328 [*Izv., Atmos. Ocean. Phys.* (Engl. Transl.), 1999, vol. 35, no. 3, pp. 291–297].
11. Carbary, J.F., Darlington, E.H., Harris, T.J., McEvaddy, P.J., Mayr, M.J., Peacock, K., and Meng, C.I., *Ultraviolet and Visible Imaging and Spectrographic Imaging Instrument*, *Appl. Opt.*, 1994, vol. 33, no. 19, pp. 4201–4213.
12. Paxton, L.J., Meng, C.I., Anderson, D.E., and Romick, G.J., *MSX—Multicourse Space Experiment*, *Johns Hopkins APL Tech. Dig.*, 1996, vol. 17, no. 1, pp. 19–33.
13. Korpela, S. *et al.*, *GOMOS, Global Ozone Monitoring by Occultation of Stars*, *Proc. Quadrennial Ozone Symp., 1988*, Hampton, Virginia: Deepak, 1992, p. 11695.
14. Popescu, A.F. and Paulsen, T., *The Global Ozone Monitoring by Occultation of Stars (GOMOS) Instrument on ENVISAT; Requirements, Design and Development Status*, *ESAMS99*, vol. 1, pp. 89–99.
15. Gurvich, A.S., Kon, A.I., Mironov, V.L., and Khmelevtsov, S.S., *Lazernoe izluchenie v turbulentnoi atmosfere* (Laser Radiation in a Turbulent Atmosphere), Moscow: Nauka, 1967.
16. Grechko, G.M., Gurvich, A.S., and Romanenko, Yu.V., *Structure of Stratospheric Density Irregularities According to the Observations on Board Salyut 6*, *Izv. Akad. Nauk SSSR, Fiz. Atmos. Okeana*, 1980, vol. 16, no. 4, pp. 339–344.
17. Aleksandrov, A.P., Grechko, G.M., Gurvich, A.S., Kan, V., Manarov, M.Kh., Pakhomov, A.I., Romanenko, Yu.V., Savchenko, S.A., Serova, S.I., and Titov, V.G., *Spectra of the Stratospheric Temperature Variations according to Stellar Scintillation Observations from Space*, *Izv. Akad. Nauk SSSR, Fiz. Atmos. Okeana*, 1990, vol. 26, no. 1, pp. 5–16.
18. Grechko, G.M., Gurvich, A.S., Kan, V., Pakhomov, A.I., Podvyaznyi, Ya.P., and Savchenko, S.A., *Observations of the Atmospheric Turbulence at Altitudes of 20–70 km*, *Dokl. Ross. Akad. Nauk*, 1997, vol. 357, no. 5, pp. 683–686.
19. *Spravochnik po geofizike* (A Handbook for Geophysics), Moscow: Nauka, 1965.
20. Grechko, G.M., Gurvich, A.S., Kan, V., Sokolovskiy, S.V., and Savchenko, S.A., *Scintillations and Random Refraction during Occultations by Terrestrial Atmosphere*, *J. Opt. Soc. Am. A*, 1985, vol. 2, no. 12, pp. 2120–2123.
21. Born, M. and Wolf, E., *Principles of Optics*, Oxford: Pergamon, 1969. Translated under the title *Osnovy optiki*, Moscow: Nauka, 1970, Chapter 4.
22. Kravtsov, Yu.A. and Orlov, Yu.A., *Geometricheskaya optika neodnorodnykh sred* (Geometrical Optics of Inhomogeneous Media), Moscow: Nauka, 1980.
23. Dalaudier, F., Kan, V., and Gurvich, A.S., *Chromatic Refraction during Star Occultations with GOMOS. Part 1: Description and Scintillation Correction*, *Appl. Opt.*, 1999 (submitted).
24. Kan, V., Dalaudier, F., and Gurvich, A.S., *Chromatic Refraction during Star Occultations with GOMOS. Part 2: Statistical Properties of Scintillations*, *Appl. Opt.*, 1999 (submitted).
25. Gurvich, A.S. and Kan, V., *Radio Wave Fluctuations in Satellite–Atmosphere–Satellite Links: Estimates from Stellar Scintillation Observations and Their Comparison with Experimental Data*, *Izv. Ross. Akad. Nauk, Fiz. Atmos. Okeana*, 1997, vol. 33, no. 3, pp. 314–323 [*Izv., Atmos. Ocean. Phys.* (Engl. Transl.), 1997, vol. 33, no. 3, pp. 284–292].
26. Sidi, C. and Dalaudier, F., *Temperature and Heat Flux Spectra in the Turbulent Buoyancy Subrange*, *PAGEOPH*, 1989, vol. 130, nos. 2–3, pp. 547–569.
27. Tsuda, T., VanZandt, T.E., Mizumoto, M., Kato, S., and Fukao, S., *Spectral Analysis of Temperature and Brunt–Väisälä Frequency Fluctuations Observed by Radiosondes*, *J. Geophys. Res. D*, 1991, vol. 96, no. 9, pp. 17265–17278.
28. Rytov, S.M., Kravtsov, Yu.A., and Tatarskii, V.I., *Vvedenie v statisticheskuyu radiofiziku* (Introduction to Statistical Radiophysics), Moscow: Nauka, 1978, part 2.
29. Kandidov, V.P., *Monte Carlo Method in Nonlinear Statistical Optics*, *Usp. Fiz. Nauk*, 1996, vol. 166, no. 12, pp. 1309–1338.
30. Turchin, V.F., Kozlov, V.P., and Malkevich, M.S., *Use of Mathematical Statistics Methods to Solve Ill-Posed Problems*, *Usp. Fiz. Nauk*, 1970, vol. 102, no. 3, pp. 345–386.

*Translated by B. Dribinskaya*